Geometrical Tunability of Linear Optical Response of Silica−Gold Double Concentric Nanoshells

Ovidio Peña-Rodríguez*,† and Umapada Pal‡

Institut de Ciència de Materials de Barcelona, Campus UAB, Bellaterra, Barcelona, 08193, España, and Instituto de Física, Universidad Autónoma de Puebla, Apartado Postal J-48, Puebla, Puebla 72570, México

Received: January 5, 2010; Revised Manuscript Received: February 12, 2010

Linear optical responses of double concentric nanoshells (DCN), consisting of two alternating layers of dielectric and metal, are studied using the Mie theory and plasmon hybridization theory. Reduction of thickness either of the metallic layers or the second dielectric layer produces red-shifts of the $|\omega_{-}^{-}\rangle$ energy mode. A combined manipulation of these parameters can achieve an even greater shift of the surface plasmon resonance band toward the near-infrared region, favorable for biological applications. It has been demonstrated that these DCN structures have a greater geometrical tunability than the metallic nanoshells and metal−dielectric−metal structures of similar dimensions.

1. Introduction

Metal nanoparticles (NPs) have generated great interest at present due to their unique electronic and optical properties, which are dominated by the surface plasmon resonance (SPR), defined as collective oscillations of the free electrons. The SPR frequency of metal nanoparticles, which depends on their size, shape, structure, and composition,[1] along with the nature of dispersing dielectric medium, can be varied over a wide range by changing the above-mentioned parameters. Particularly metallic nanoshells[2,3] and their variants[4–6] have received a lot of attention recently. Even though this kind of structures has a simple shape, they present notable structural tunability of the plasmon frequencies, as has been shown both theoretically[2] and experimentally.[7]

Though Ag presents the most intense SPR among the noble metals, it readily oxidizes in air and has a poor biocompatibility. For this reason, in spite of the outstanding optical properties of Ag, Au is the preferred material for fabricating metallic nanoshells for biological applications.[3] Additionally, the chemical processes for synthesizing Au nanoshells are well-known and easier, which allow the control of size of the core and thickness of the shell.[8] For various applications like in medical diagnostics,[9] immunoassay,[10,11] and studies of living cells and bacteria,[12] it is necessary to shift the SPR to the near-infrared region (800−1200 nm) where the biological tissues are transparent.[10] This can be achieved by decreasing the ratio between the thickness of the metallic shell and the total radius[2] of the NPs. However, while the reduction of thickness of the metal layer induces a very weak near-field, increase in particle size enhances the absorption coefficient. Both factors are unfavorable for applications such as surface-enhanced spectroscopy and thermal therapy of tumors.[13] Moreover, for some applications smaller nanoparticles are preferred. For instance, for using NPs as contrasting agents in biomedicine, it is important to reduce the diameter of the particles to a few tens of nanometers to facilitate their penetration into the biological tissues.

A simple, yet effective alternative to single nanoshells can be the structures with additional metallic layers, which can produce additional red-shifts through plasmon hybridization, while maintaining the small size and strong surface plasmon resonance. For example, metal−dielectric−metal (MDM) hybrid nanostructures have been synthesized[14] and studied theoretically[5,15] in recent years, with excellent results. Nevertheless, in our opinion, an even better alternative is double concentric nanoshells (DCN), consisting of two alternating layers of dielectric and metal. An additional advantage of DCNs over the MDM structures lies in the tunability of the SPR of their inner shells (in contrast to the plasmon of a sphere, which is essentially fixed). Therefore, the size of the particles could be further reduced without affecting their optical properties. Synthesis of such structures should be no harder than that of the MDM ones and indeed they have already been synthesized,[4,6] albeit for a different purpose. However, apart from those pioneer works, little attention has been paid to those structures, and to the best of our knowledge, there is no reported study on the influence of the geometry over the optical response of double concentric nanoshells.

In this article, we have used classical Mie calculations[16–18] to study the influence of the inner and outer nanoshells and the middle dielectric layer on the SPR behaviors of DCNs. The bulk values of Au dielectric function reported by Johnson and Christy[19] were used for the calculations, after applying a size correction.[2] It was found that DCNs can have smaller sizes than MDM structures to maintain equivalent excellent near-infrared properties. The obtained results were explained in terms of the theory of plasmon hybridization. DCNs could provide an excellent replacement for both nanoshells and MDM structures as contrasting agents that can generate a tunable SPR peak in the spectral region well suited for optical bioimaging and biosensing applications.

2. Procedure

Several theoretical approaches have been developed to characterize the features of the SPR of metallic structures. For instance, the analysis of SPR properties of spherical metallic nanoparticles is usually done by means of the Mie theory,[16,17] as it allows obtaining the exact solution of Maxwell's equations

* To whom correspondence should be addressed. E-mail: ovidio@bytesfall.com.
† Institut de Ciència de Materials de Barcelona.
‡ Universidad Autónoma de Puebla.

10.1021/jp1001034
Published on Web 02/23/2010

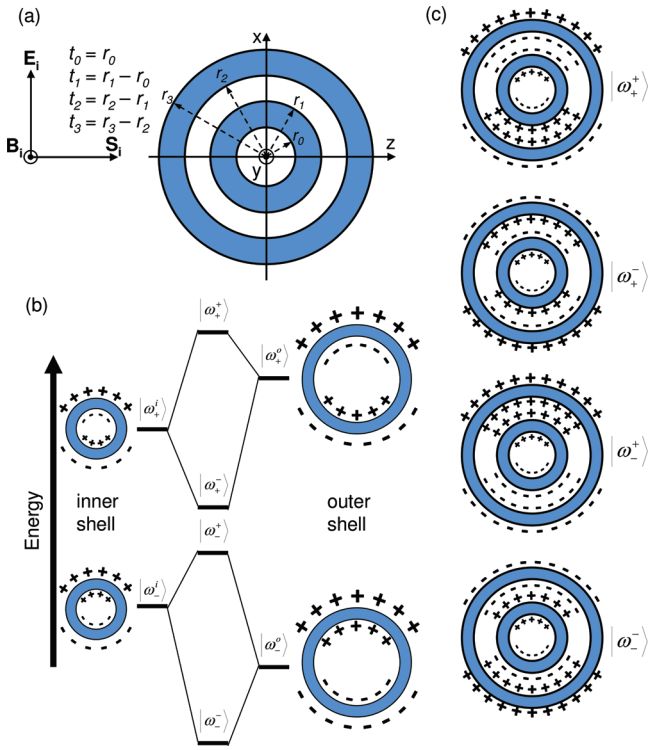

Figure 1. Schematic representation of a double concentric nanoshell (a), its corresponding energy diagram, representing plasmon hybridization (b), and the induced polarizations of the DCN modes (c).

in spherical coordinates with appropriate boundary conditions. The theory of plasmon hybridization[6] has also been developed to study the SPR of metallic nanoparticles. In this theory, the characteristics of the SPR are explained in terms of the interaction between the plasmons of metallic nanostructures in simpler forms. For example, the SPR of metallic nanoshells can be viewed as the interaction between the plasmons of a sphere and a cavity. The hybridization of the plasmon of the sphere and the cavity creates two new plasmon oscillation modes, i.e., the higher energy (antibonding) mode $|\omega_+\rangle$ and the lower energy (bonding) mode $|\omega_-\rangle$, corresponding to the antisymmetric and symmetric interactions between the $|\omega_s\rangle$ and $|\omega_c\rangle$ modes, respectively.

In this work we have studied double concentric nanoshells with geometries as shown in Figure 1a. The extinction efficiencies for the different configurations were calculated by using the computer software scattnlay,[18] which is an implementation of the algorithm developed by Yang[20] for a multilayered sphere. The obtained shifts of the SPR are explained in terms of plasmon hybridization theory.

The energy level diagram for plasmon hybridization in the studied DCNs is depicted in Figure 1b. The plasmon resonance in a DCN can be considered as the interaction between the plasmon responses of the inner ($|\omega^i_-\rangle$ and $|\omega^i_+\rangle$) and outer ($|\omega^o_-\rangle$ and $|\omega^o_+\rangle$) nanoshells. The energy mode $|\omega^-_-\rangle$ ($|\omega^+_-\rangle$) corresponds to the antisymmetric (symmetric) coupling between the symmetric plasmon resonance modes of the inner ($|\omega^i_-\rangle$) and outer ($|\omega^o_-\rangle$) nanoshells. On the other hand, the energy mode $|\omega^-_+\rangle$ ($|\omega^\pm_+\rangle$) corresponds to the symmetric (antisymmetric) coupling between the antisymmetric plasmon resonance modes of the inner ($|\omega^i_+\rangle$) and outer ($|\omega^o_+\rangle$) nanoshells (Figure 1c). The higher energy of the $|\omega^\pm_-\rangle$ and $|\omega^\pm_+\rangle$ modes, in comparison to the corresponding modes of the single nanoshells, is due to the increased electrostatic repulsion at the internal adjacent interfaces of the particle, occurring for those plasmon excitations.[4]

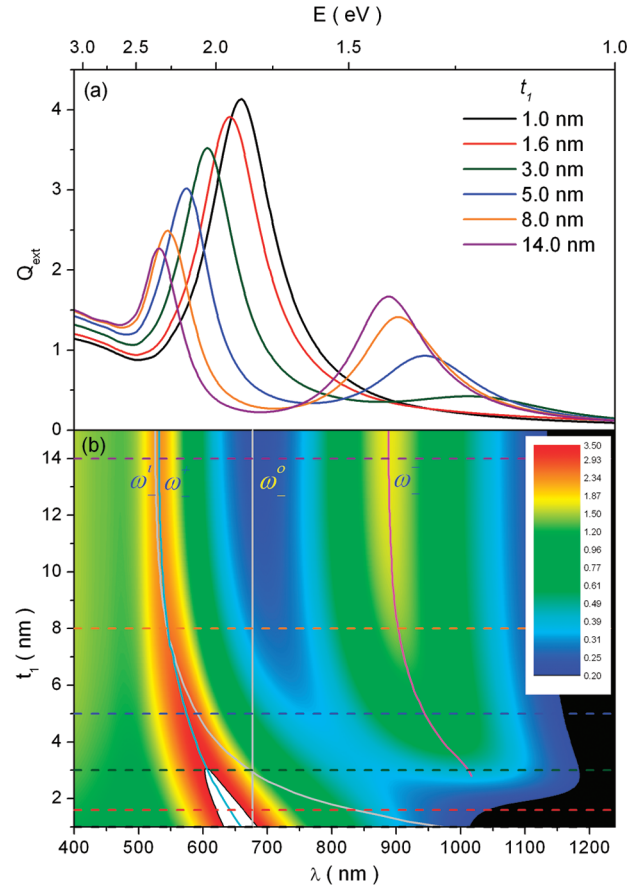

Figure 2. Simulated extinction efficiency for a DCN, having $t_2 = t_3 = 5.0$ nm, and $t_0 + t_1 = 16.0$ nm, while t_1 varied between 1.0 and 15.0 nm. For clarity, Q_{ext} is presented for some selected values of t_1 (a) and for the whole interval (b).

Although, in principle, there exists also a coupling between the antisymmetric and symmetric plasmons of the separate nanoshells, it has only a small influence on the hybridized modes, due to the large energy separation between those two modes.[6] As can be seen in the following section, similar to the plasmon hybridization in metallic nanoshells[21] and metal−dielectric−metal structures,[5] the $|\omega^-_-\rangle$ mode is usually more sensitive to the symmetric mode of the outer nanoshell, while the $|\omega^\pm_-\rangle$ mode is more dependent on the symmetric mode of the inner one. However, there are regions where the opposite is also true.

3. Results and Discussion

Figure 2 shows the calculated extinction efficiency (Q_{ext}) spectrum for the first case, where the thicknesses of the third and fourth shells (t_2 and t_3) are fixed to 5.0 nm and $t_0 + t_1 = 16.0$ nm, while t_1 varies between 1.0 and 15.0 nm. Therefore, in this configuration both $|\omega^o_-\rangle$ and the coupling strength are fixed, and all the changes in the hybridized modes are driven by $|\omega^i_-\rangle$. The details of the variation of Q_{ext} with the wavelength and t_1 can be observed in Figure 2b. For a very thin layer ($t_1 \approx 1$ nm) the bonding mode is practically indistinguishable and considerably red-shifted. The antibonding mode, on the other hand, is a strong peak, slightly blue-shifted with respect to $|\omega^o_-\rangle$. As t_1 gets thicker, both the modes get blue-shifted until $t_1 \approx 10$ nm, and then they become almost constant. From the results it is evident that in this case both hybridized modes are affected by the variations of $|\omega^i_-\rangle$ in a similar way. Additionally, it can be observed that the hybridization of the plasmon is symmetric for a thin inner layer but becomes asymmetric when it becomes

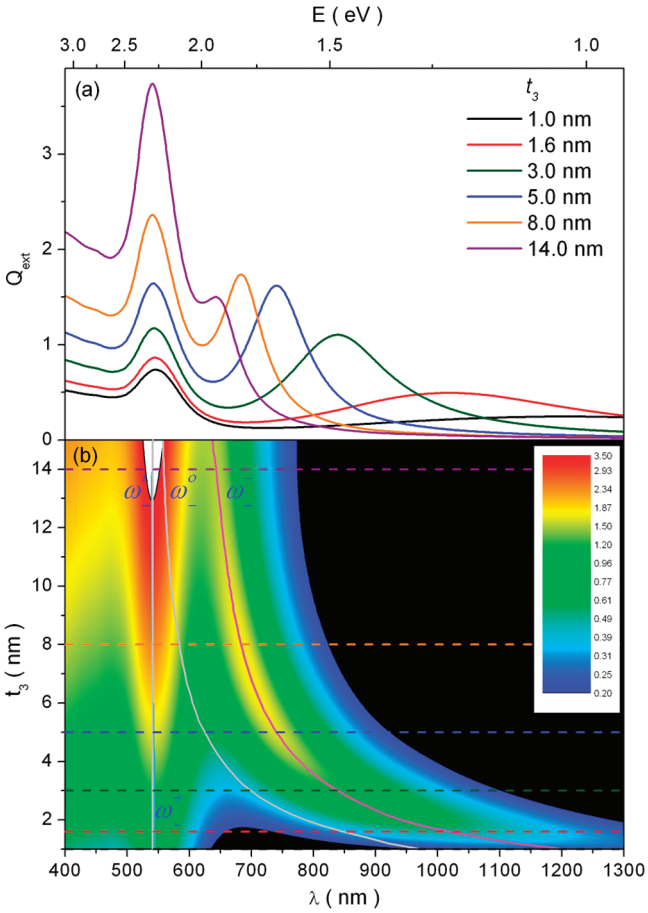

Figure 3. Simulated extinction efficiency for a DCN, having $t_0 = t_1 = t_2 = 5.0$ nm, while t_3 is varied between 1.0 and 15.0 nm. For clarity, Q_{ext} is presented for some selected values of t_3 (a) and for the whole interval (b).

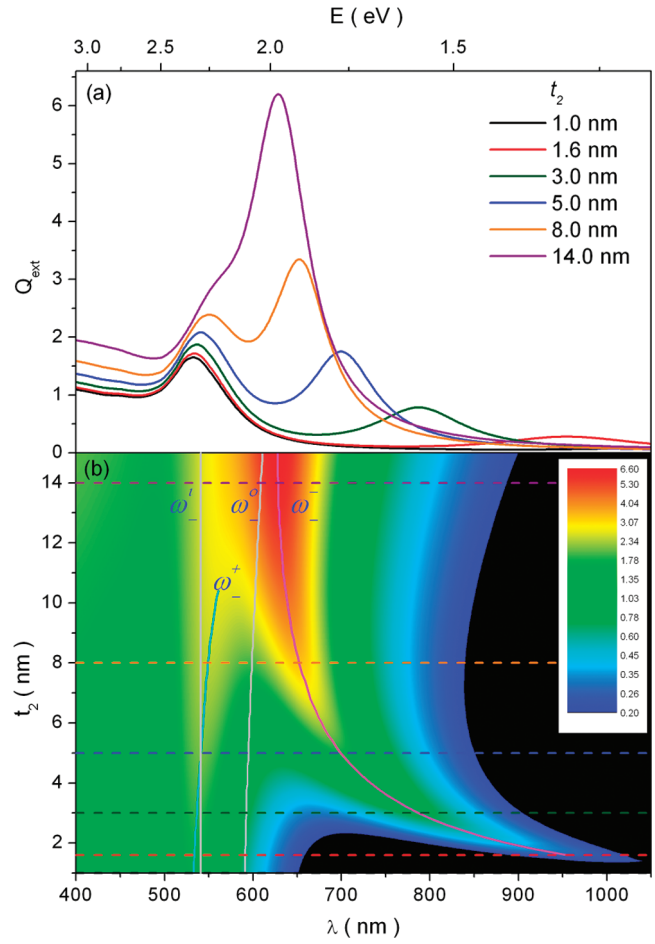

Figure 4. Simulated extinction efficiency for a DCN, having $t_0 = t_1 = 5.0$ nm, while t_2 is varied between 1.0 and 15.0 nm. The value of t_3 was calculated for each t_2 from the relation $t_3/r_3 = 5/16$. For clarity, Q_{ext} is presented for some selected values of t_2 (a) and for the whole interval (b).

thicker. The asymmetric hybridization for a thicker inner layer is produced mainly due to phase-retardation effects[5,6] and the small but finite interaction with the higher energy $|\omega^{i}_{+}\rangle$ and $|\omega^{o}_{+}\rangle$ plasmon modes.[6] The influence of $|\omega^{o}_{-}\rangle$ on the hybridized SPR was also analyzed in the second case (Figure 3). Here the first three layers were fixed ($t_0 = t_1 = t_2 = 5.0$ nm) and t_3 was varied between 1.0 and 15.0 nm. For this case, the bonding mode of the outer shell remained always at lower energy than its counterpart for the inner shell. As a result, the positions of $|\omega^{-}_{-}\rangle$ and $|\omega^{+}_{-}\rangle$ are almost completely defined by the modes of the inner and outer shell, respectively.

Likewise, the influence of the intermediate silica layer on the hybridized modes was studied (Figure 4). For this purpose, the thicknesses of the first two layers were kept fixed ($t_0 = t_1 = 5.0$ nm), and t_2 was varied between 1.0 and 15.0 nm. A little bit trickier t_3 value was selected for this case. As for nanoshells the position of SPR depends only on the t/R_{Shell} ratio,[2,22] for each t_2 value, the values of t_3 were calculated considering $t_3/r_3 = 5/16$. It is worth noting that the value of $|\omega^{o}_{-}\rangle$ varied a little for the variation of t_2 from 1.0 to 15.0 nm, as a consequence of the increase in particle size. However, we consider that this has no influence on the observed behaviors of $|\omega^{-}_{-}\rangle$ and $|\omega^{+}_{-}\rangle$. While the $|\omega^{+}_{-}\rangle$ mode was not heavily affected due to the variation of intermediate layer thickness (t_2), the $|\omega^{-}_{-}\rangle$ mode drastically red-shifted on reducing t_2, which is a direct consequence of the increased coupling between the bonding modes of both metallic nanoshells. For the given example, the intensity of the $|\omega^{-}_{-}\rangle$ mode also decreased considerably on reducing the value of t_2. We believe the decrease of intensity of the $|\omega^{-}_{-}\rangle$ mode is mainly due to the small value of t_3, used to keep the position of $|\omega^{o}_{-}\rangle$ fixed, not an effect of the increased coupling. The greater the value of t_2, the lower the coupling between the shells, resulting an increased (decreased) resonance energy for the $|\omega^{-}_{-}\rangle$ ($|\omega^{+}_{-}\rangle$) mode, tending both modes close to the value of $|\omega^{o}_{-}\rangle$.

Figure 5 shows the extinction efficiency corresponding to a DCN where the thicknesses of the silica layers were kept fixed ($t_0 = t_2 = 5$ nm) and the thicknesses of the gold layers were varied ($t_1 = 1, 2, ..., 15$ nm; $t_3 = 16$ nm $- t_1$) to have an opposite behavior between the modes of the inner and outer shells. As expected, for bigger values of t_1 (small t_2) the $|\omega^{+}_{-}\rangle$ mode remained almost constant and the $|\omega^{-}_{-}\rangle$ mode was mainly driven by the outer shell. For the smaller values of t_1 (big t_2), contrary to what one would expect, the bonding hybridized mode instead of red-shifting, keeps blue-shifting until it almost disappears, "absorbed" by the antibonding one. This phenomenon can be explained considering the shielding caused by the thick outer layer, through which the light does not "see" the inner layer; and therefore, the particle behaves almost like a single nanoshell.

Finally, Figure 6 compares the optical density (calculated for a fluence f of 1.0×10^{17} atoms/cm^2, in the same way that we have described before[23]) of a DCN with a MDM particle ($t_0 = 0$) and a nanoshell ($t_0 = t_1 = 0$) for two different cases: particles with the same shell thicknesses in the first case and with the same total volume in the second case. In both cases the calculations were performed for particles having the same thicknesses in all of its layers. In this way, all the thicknesses

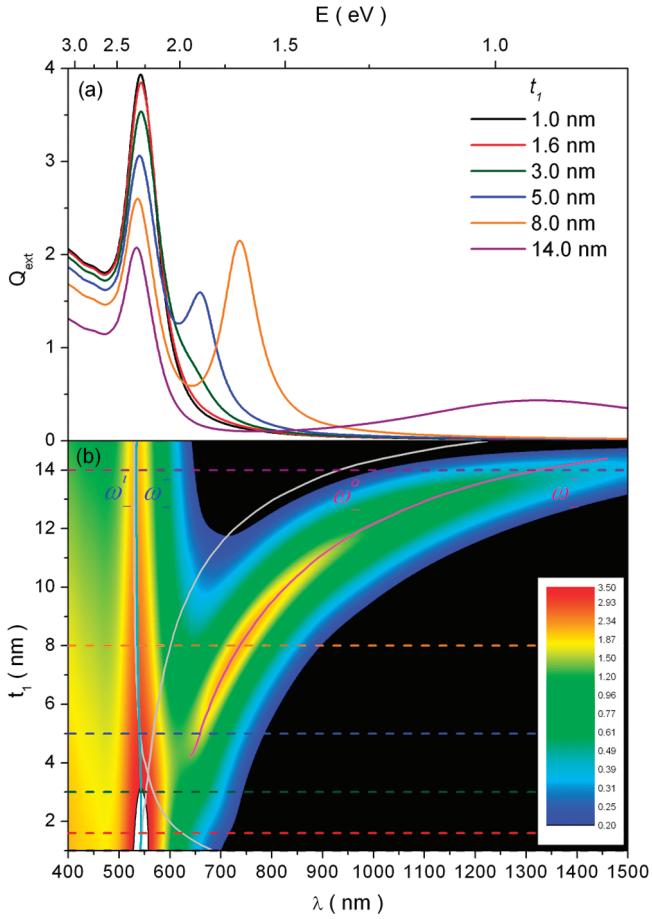

Figure 5. Simulated extinction efficiency for a DCN, having $t_0 = t_2 = 5$ nm, while t_1 and t_3 are varied ($t_1 = 1, 2, ..., 15$ nm; $t_3 = 16$ nm $- t_1$) simultaneously. For clarity, Q_{ext} is presented for some selected values of t_1 (a) and for the whole interval (b).

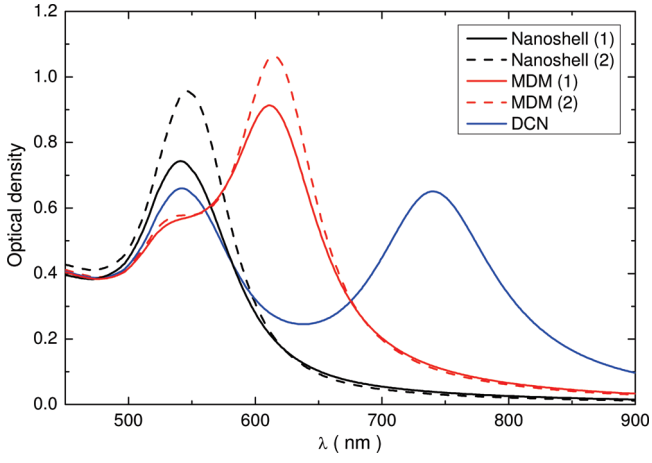

Figure 6. Comparison of SPR shifts of a DCN, with the equivalent nanoshells ($t_0 = t_1 = 0$) and MDM structures ($t_0 = 0$) for particles with the same shell thicknesses (solid lines) and with the same total volume (dashed lines). All the thicknesses were equal to 5.0 nm in the first case while in the second one $t_2 = t_3 = 10.0$ nm for the nanoshell, $t_1 = t_2 = t_3 = 6.667$ nm for the MDM, and all the thicknesses remained equal to 5.0 nm for the DCN.

were equal to 5.0 nm in the first case while in the second one $t_2 = t_3 = 10.0$ nm for the nanoshell, $t_1 = t_2 = t_3 = 6.667$ nm for the MDM, and all the thicknesses remained equal to 5.0 nm for the DCN. We can clearly see that the DCN can achieve major SPR red-shifts either for the same thicknesses or for the same total volume when compared to a nanoshell or a MDM structure. In both cases the intensity of the red-shifted SPR peak for the DCN is lower but nevertheless it should be intense enough for most applications.

4. Conclusions

In this paper we have studied the characteristics of the SPR of double concentric nanoshells by means of the Mie theory. With a decrease in the thickness of the inner gold shell (with second radius r_1 fixed) both the hybridized modes of the DCN are considerably red-shifted and the $|\omega^-\rangle$ one can be easily placed in the near-infrared region. A similar behavior is observed for the bonding mode for a reduction in t_3 but in this case the antibonding mode remains unaffected. The thickness of the middle silica layer also plays an important role, since it controls the strength of the coupling between the modes of both metallic layers. Double concentric nanoshells are better suited over metallic nanoshells and metal−dielectric−metal structures for biological applications due to their better tunability of the SPR bands.

References and Notes

(1) Kelly, K. L.; Coronado, E.; Zhao, L. L.; Schatz, G. C. *J. Phys. Chem. B* **2003**, *107*, 668–677.
(2) Peña, O.; Pal, U.; Rodríguez-Fernández, L.; Crespo-Sosa, A. *J. Opt. Soc. Am. B* **2008**, *25*, 1371–1379.
(3) Oldenburg, S. J.; Jackson, J. B.; Westcott, S. L.; Halas, N. J. *Appl. Phys. Lett.* **1999**, *75*, 2897–2899.
(4) Radloff, C.; Halas, N. J. *Nano Lett.* **2004**, *4*, 1323–1327.
(5) Wu, D.; Liu, X. *Appl. Phys. B: Lasers Opt.* **2009**, *97*, 193–197.
(6) Prodan, E.; Radloff, C.; Halas, N. J.; Nordlander, P. *Science* **2003**, *302*, 419–422.
(7) Schwartzberg, A. M.; Olson, T. Y.; Talley, C. E.; Zhang, J. Z. *J. Phys. Chem. B* **2006**, *110*, 19935–19944.
(8) Oldenburg, S. J.; Averitt, R. D.; Westcott, S. L.; Halas, N. J. *Chem. Phys. Lett.* **1998**, *288*, 243–247.
(9) Allain, L. R.; Vo-Dinh, T. *Anal. Chim. Acta* **2002**, *469*, 149–154.
(10) Hirsch, L. R.; Jackson, J. B.; Lee, A.; Halas, N. J.; West, J. L. *Anal. Chem.* **2003**, *75*, 2377–2381.
(11) Cui, Y.; Ren, B.; Yao, J.; Gu, R.; Tian, Z. *J. Phys. Chem. B* **2006**, *110*, 4002–4006.
(12) Premasiri, W. R.; Moir, D. T.; Klempner, M. S.; Krieger, N.; Jones, G.; Ziegler, L. D. *J. Phys. Chem. B* **2005**, *109*, 312–320.
(13) Hirsch, L. R.; Stafford, R. J.; Bankson, J. A.; Sershen, S. R.; Rivera, B.; Price, R. E.; Hazle, J. D.; Halas, N. J.; West, J. L. *Proc. Natl. Acad. Sci. U.S.A.* **2003**, *100*, 13549–13554.
(14) Xia, X.; Liu, Y.; Backman, V.; Ameer, G. A. *Nanotechnology* **2006**, *17*, 5435–5440.
(15) Hasegawa, K.; Rohde, C.; Deutsch, M. *Opt. Lett.* **2006**, *31*, 1136–1138.
(16) Mie, G. *Ann. Phys.* **1908**, *330*, 377–445.
(17) Bohren, C. F.; Huffman, D. R. *Absorption and scattering of light by small particles*; Wiley-Interscience: New York, 1998.
(18) Peña, O.; Pal, U. *Comput. Phys. Commun.* **2009**, *180*, 2348–2354.
(19) Johnson, P. B.; Christy, R. W. *Phys. Rev. B* **1972**, *6*, 4370.
(20) Yang, W. *Appl. Opt.* **2003**, *42*, 1710–1720.
(21) Prodan, E.; Lee, A.; Nordlander, P. *Chem. Phys. Lett.* **2002**, *360*, 325–332.
(22) Prodan, E.; Nordlander, P. *Nano Lett.* **2003**, *3*, 543–547.
(23) Peña, O.; Rodríguez-Fernández, L.; Rodríguez-Iglesias, V.; Kellermann, G.; Crespo-Sosa, A.; Cheang-Wong, J. C.; Silva-Pereyra, H. G.; Arenas-Alatorre, J.; Oliver, A. *Appl. Opt.* **2009**, *48*, 566–572.

JP1001034